Hydrogenated amorphous silicon deposited at very high growth rates by an expanding Ar-H2-SiH4 plasma

Hydrogenated amorphous silicon deposited at very high growth rates by an expanding $Ar–H_2–SiH_4$ plasma

W. M. M. Kessels,[a] R. J. Severens,[b] A. H. M. Smets, and B. A. Korevaar
Department of Applied Physics, Eindhoven University of Technology, P.O. Box 513, 5600 MB Eindhoven, The Netherlands

G. J. Adriaenssens
Semiconductor Physics Laboratory, Katholieke Universiteit Leuven, Celestijnenlaan 200 D, B3001 Heverlee-Leuven, Belgium

D. C. Schram and M. C. M. van de Sanden[c]
Department of Applied Physics, Eindhoven University of Technology, P.O. Box 513, 5600 MB Eindhoven, The Netherlands

(Received 1 March 2000; accepted for publication 14 November 2000)

The properties of hydrogenated amorphous silicon (a-Si:H) deposited at very high growth rates (6–80 nm/s) by means of a remote $Ar–H_2–SiH_4$ plasma have been investigated as a function of the H_2 flow in the $Ar–H_2$ operated plasma source. Both the structural and optoelectronic properties of the films improve with increasing H_2 flow, and a-Si:H suitable for the application in solar cells has been obtained at deposition rates of 10 nm/s for high H_2 flows and a substrate temperature of 400 °C. The ''optimized'' material has a hole drift mobility which is about a factor of 10 higher than for standard a-Si:H. The electron drift mobility, however, is slightly lower than for standard a-Si:H. Furthermore, preliminary results on solar cells with intrinsic a-Si:H deposited at 7 nm/s are presented. Relating the film properties to the SiH_4 dissociation reactions reveals that optimum film quality is obtained for conditions where H from the plasma source governs SiH_4 dissociation and where SiH_3 contributes dominantly to film growth. Conditions where ion-induced dissociation reactions of SiH_4 prevail and where the contribution of SiH_3 to film growth is much smaller lead to inferior film properties. A large contribution of very reactive (poly)silane radicals is suggested as the reason for this inferior film quality. Furthermore, a comparison with film properties and process conditions of other a-Si:H deposition techniques is presented. © *2001 American Institute of Physics.* [DOI: 10.1063/1.1338985]

I. INTRODUCTION

Among the presently investigated renewable energy sources, thin film solar cells based on hydrogenated amorphous and/or microcrystalline silicon technology are a clean and cost-effective alternative for nowadays fossil fuels. In the research to improve their price/performance ratio, special attention has been addressed in the recent years to increase the deposition rate of the intrinsic silicon layer in these solar cells. A higher deposition rate enables a higher throughput without adding more processing equipment and, consequently, large-scale production can be obtained with a reduction of the production costs.

Hydrogenated amorphous silicon (a-Si:H) is usually deposited by ''conventional'' radio frequency (13.56 MHz) plasma enhanced chemical vapor deposition (rf PECVD) at rates of 0.1–0.3 nm/s. Various efforts has been made to increase the deposition rate while maintaining (reasonable) film quality. These efforts range from investigations of more ''extreme'' operating conditions (at high power and pressure, working in the γ regime),[1,2] different reactor geometries (depositing under additional ion bombardment),[3] and other gas mixtures (admixing noble gases[4,5] or using Si_2H_6)[1,6] to develop other a-Si:H production techniques. The development of these production techniques has been initiated by the fact that the increase in deposition rate for rf PECVD is limited as it rapidly goes at the expense of the material quality. A more significant improvement has been obtained by changing the excitation frequency from 13.56 MHz to the very high frequency (VHF) range (30–300 MHz). For this VHF PECVD technique deposition rates up to 3 nm/s have been reported.[7–9] However, for the production of solar cell devices the deposition rate is in practice usually limited to rates below 1 nm/s.[10,11]

A feature of the aforementioned methods is that they are so-called ''direct plasma'' techniques. This means that plasma generation and deposition take place in the same region, which makes it difficult or impossible to vary plasma parameters independently. For this reason, in the last decade a lot of research has been devoted to remote plasma techniques, where plasma generation, growth precursor transport, and deposition are geometrically separated. Some examples are: microwave generated plasmas,[12,13] inductively coupled plasmas (ICP),[14–16] and electron cyclotron resonance (ECR) plasmas.[17–19] The deposition rates obtained by these techniques seize also up at ~1 nm/s. However, for some of the

[a]Electronic mail: w.m.m.kessels@tue.nl
[b]Present address: AKZO-NOBEL Central Research, P.O. Box 9300, 6800 SB Arnhem, The Netherlands.
[c]Electronic mail: m.c.m.v.d.sanden@tue.nl

techniques the favorable film properties obtained, such as a high stability against light-induced degradation, are of more interest.[12,19]

A technique for which both advantages, i.e., high growth rate and high stability of the *a*-Si:H deposited, have been reported is hot wire chemical vapor deposition (HWCVD). With this technique, device quality *a*-Si:H has been obtained at deposition rates in the range of 0.5–2 nm/s.[20–23] For films deposited at high substrate temperatures (~400 °C) good electronic properties have been obtained[20,21] while films with a low H content (2–3 at. %) exhibit improved stability against light-induced degradation.[24,25] This property, together with the very different electronic and structural properties,[26–28] are most probably related to the specific growth conditions of HWCVD, such as a high flux of H, a high substrate temperature, and a lack of energetic particle bombardment.[20]

This article describes high rate deposition of *a*-Si:H using the expanding thermal plasma (ETP). For this remote plasma deposition technique, it has recently been shown that it can produce good quality *a*-Si:H at deposition rates up to 10 nm/s.[29–31] The technique uses a, in a subatmospheric plasma source created, $Ar–H_2$ plasma for SiH_4 dissociation in a low-pressure deposition chamber. In this article, the film properties of the *a*-Si:H deposited will be presented as a function of the H_2 flow in the plasma source and for two different substrate temperatures.

The aim of this article is not only to show that *a*-Si:H with properties suitable for the application in solar cells can be deposited at rates up to 10 nm/s, but also to relate the *a*-Si:H properties to the plasma processes and to the contribution of different plasma species to film growth. The production of Si containing ions and radicals and their contribution to film growth in the expanding thermal plasma has been studied in detail by the combination of different plasma diagnostics and has been presented in previous work.[32–37] It has been observed that the plasma processes in the downstream region change drastically when varying the H_2 flow in the plasma source. The dominant SiH_4 dissociation process shifts from ion-induced reactions at zero or low H_2 flows to H abstraction reactions of SiH_4 by H atoms at higher H_2 flows.[32,35,37] This causes a transition from film growth with a large contribution of very reactive (poly)silane radicals at low H_2 flows to film growth with a dominant contribution of SiH_3 radicals at higher H_2 flows.[37] A small contribution of H-poor cationic Si clusters remains rather constant as a function of the H_2 flow.[35] The consequences of this transition in growth precursors for the *a*-Si:H film properties will be presented and possible relations indicated.

From this study, more insight into the growth of good quality *a*-Si:H at high deposition rates can be obtained while the results are also relevant for other (low-deposition rate) techniques. From a comparison of the ETP deposited *a*-Si:H with *a*-Si:H deposited by rf PECVD and other techniques (HWCVD/other remote plasmas), it is tried to come to general insights with respect to *a*-Si:H deposition. For example, from similarities in film properties and growth conditions it is possible to address questions such as: ''What is the role of ion bombardment?,'' ''Are high substrate temperatures inevitable for obtaining good quality *a*-Si:H at high deposition rates?,'' etc.

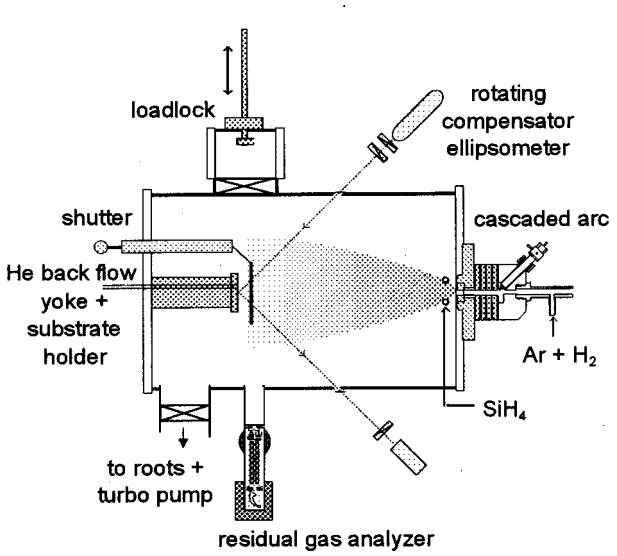

FIG. 1. Schematic representation of the ETP deposition system.

II. DEPOSITION SETUP AND FILM DIAGNOSTICS

The ETP deposition technique is schematically represented in Fig. 1. The technique is based on the generation of an $Ar–H_2$ plasma in a thermal plasma source (a cascaded arc), which subsequently expands into a low-pressure chamber where it dissociates the injected SiH_4 gas. The cascaded arc is operated at a dc current of 45 A and a voltage between 70 and 140 V depending on the H_2 fraction in the gas mixture. The Ar flow used is 55 sccs (standard cm^3s^{-1}), while the H_2 flow is varied between 0 and 15 sccs. The plasma source pressure is about 400 mbar. Pure SiH_4 is admixed in the low-pressure (0.2 mbar) chamber just behind the source exit by means of an injection ring. The SiH_4 flow is fixed at 10 sccs for the present study.[38]

Up to three substrates can be mounted on a substrate holder, which is placed on a copper yoke in the deposition chamber by means of a loadlock system. The yoke is positioned at 35 cm from the cascaded arc outlet and is resistively heated. Accurate substrate temperature control (100–500 °C) is achieved by means of a He backflow between the yoke and the substrate holder, and between the substrate holder and the substrates.[39] For the present study, substrate temperatures T of 250 and 400 °C have been used. During plasma ignition and admixing of SiH_4, the substrates are screened from the plasma by means of a shutter, which is opened after stabilization of the gases. More details on the deposition setup can be found in Refs. 32 and 35.

Films with a thickness between 500 and 1000 nm have been deposited on $2.5\times2.5\,cm^2$ *p*-type Si(111) substrates (10–20 Ω cm) and on Corning 7059 glass. The refractive index and deposition rate of the films have been obtained by *in situ* ellipsometry (at 632.8 nm) and *ex situ* infrared transmission spectroscopy. From the analysis of the ellipsometry data using an optical model for the film, also the surface roughness of the films during deposition has been

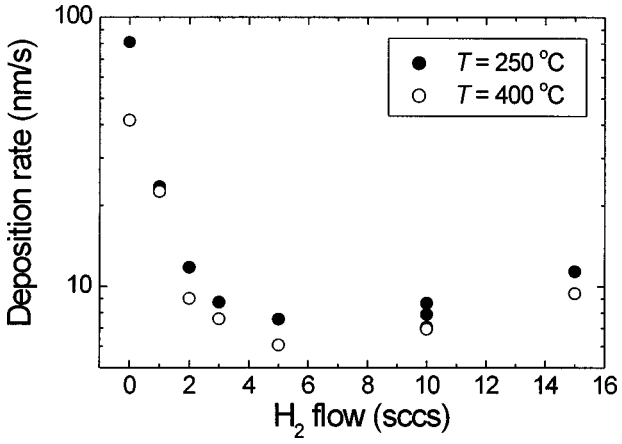

FIG. 2. Deposition rate, determined by *ex situ* infrared transmission spectroscopy and *in situ* ellipsometry, as a function of the H_2 flow in the cascaded arc plasma source for two substrate temperatures.

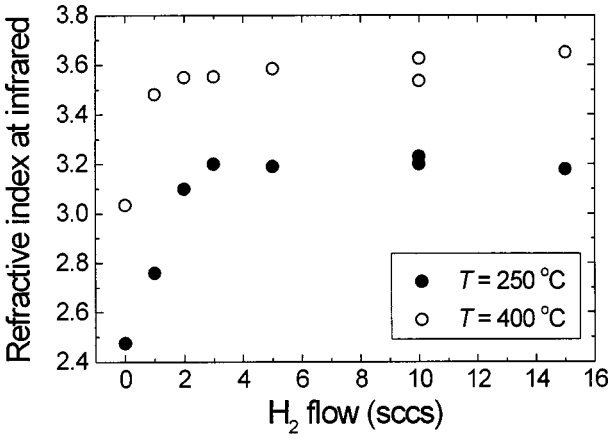

FIG. 3. Refractive index of the films as determined from *ex situ* infrared transmission spectroscopy.

obtained.[40,41] In the model, the surface roughness is represented by a toplayer with a void fraction of 50%. The H content of the films has been determined from the Si–H absorption peaks in the infrared transmission data using recalibrated values of the proportionality constants:[42] $(1.6\pm0.2)\times10^{19}\,\mathrm{cm}^{-2}$ for the wagging mode at $\sim640\ \mathrm{cm}^{-1}$, $(9.0\pm1.0)\times10^{19}\,\mathrm{cm}^{-2}$ and $(1.5\pm0.2)\times10^{20}\,\mathrm{cm}^{-2}$ for the stretching modes at ~2000 and $\sim2100\ \mathrm{cm}^{-1}$, respectively. The intensity of the absorption I for the two stretching modes has been used to calculate the microstructure parameter $R^*=I_{2100}/(I_{2000}+I_{2100})$. This yields information on how the H is bonded, as isolated SiH (absorption centered at $\sim2000\ \mathrm{cm}^{-1}$) or as SiH_2 and/or clustered SiH on internal surfaces (absorption centered at $\sim2100\ \mathrm{cm}^{-1}$). Raman spectroscopy with 514.5 nm laser radiation of an Ar^+ laser has been applied to investigate the lattice disorder.

Concerning the optoelectronic properties, the photoconductivity σ_{ph} has been obtained under air mass (AM) 1.5 illumination (100 mW/cm^2) using coplanar A1 contacts. The dark conductivity σ_d and its activation energy E_{act} have been determined in vacuum during the cool down stage after annealing the films at 160 °C for 30 min. Transmission-reflection spectroscopy has been used for the analysis of the optical band gap. The Tauc optical band gap E_{Tauc} has been determined from Tauc's equation $(\alpha E)^{1/2}=B(E-E_{Tauc})$ and the Klazes' or cubic band gap E_{cubic} from the Klazes' equation $(\alpha E)^{1/3}=C(E-E_{cubic})$ with B and C material dependent constants.[43] The electron and hole drift mobilities have been obtained from standard time-of-flight (TOF) experiments[44] using 2–4-μm-thick a-Si:H films sandwiched between a bottom Cr substrate and a top semitransparent Cr contact. The electric field applied has been varied between $(0.5\ \text{and}\ 2.5)\times10^4\,\mathrm{V\,cm}^{-1}$ for these measurements.

III. RESULTS

A. Deposition rate and structural film properties

Figure 2 shows the deposition rate of the films deposited at substrate temperatures of 250 and 400 °C for different H_2 flows in the cascaded arc plasma source. The deposition rate shows first a steep decrease as a function of the H_2 flow, followed by a slight increase at higher H_2 flows. This behavior is addressed in other articles,[32,35,37] where it was shown that at low H_2 flows SiH_4 dissociation is governed by ion-induced reactions and at high H_2 flows by reactions with atomic H from the plasma source. The deposition rate varies between 6 and 80 nm/s and is much higher than for other deposition techniques. The deposition rate also shows a dependence on the substrate temperature, especially at low H_2 flows. This can mainly be attributed to differences in film density as can be concluded from Fig. 3, where the refractive index of the films is given. The Si density or mass density is about linear in the refractive index of the films in the infrared.[42] After correcting for the film density, the deposition rate in terms of Si atoms deposited per unit of time shows only a slight decrease as a function of the substrate temperature.[36] In addition to the fact that the refractive index depends on the substrate temperature, it depends also on the H_2 flow. At low H_2 flows the refractive index is considerably lower meaning that these films contain more H and/or have a considerable void fraction.

Figure 4 shows that the H content of the films deposited at 250 °C is higher than for the films deposited at 400 °C, which is in agreement with the difference in refractive index.

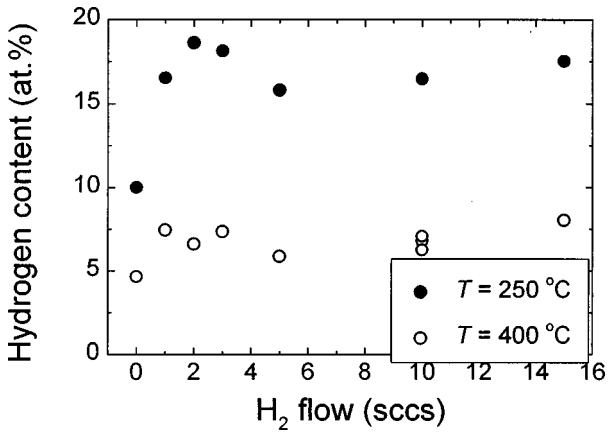

FIG. 4. The H content of the films determined from the Si–H infrared absorption peaks.

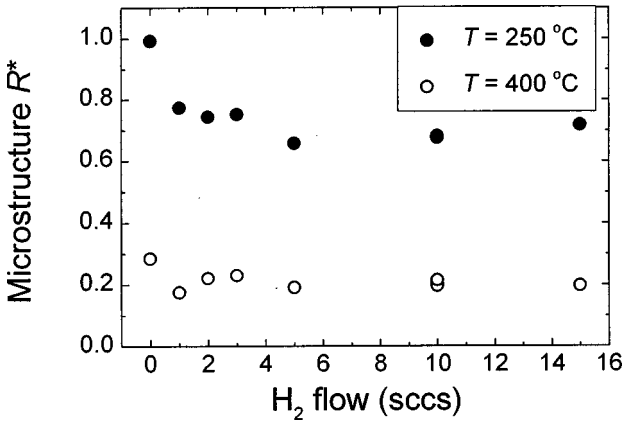

FIG. 5. The microstructure R^* as determined from the ratio of the integrated absorbance at the 2100 and 2000 cm^{-1} Si–H stretching modes.

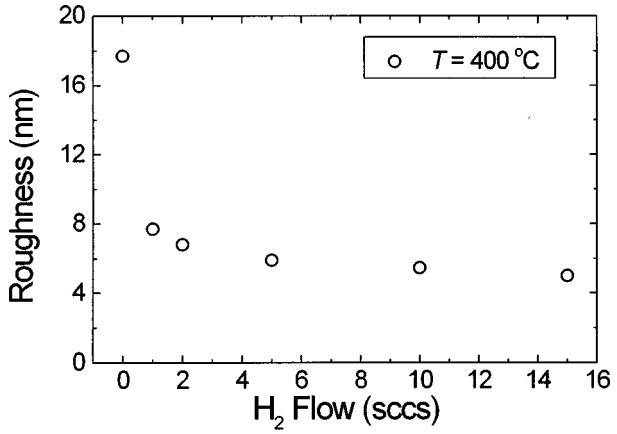

FIG. 6. The surface roughness at a film thickness of 500 nm as determined by *in situ* ellipsometry for films deposited at 400 °C. The roughness has been derived from the ellipsometry data using an optical model of the film in which the surface roughness corresponds with a toplayer containing 50% voids.

For the films deposited at 250 °C the H content is about 17 at. %, while it is about 7 at. % for the films deposited at 400 °C. The microstructure parameter R^*, given in Fig. 5, reveals that mainly the amount of H bonded as clustered SiH and/or SiH_2[45] decreases with increasing temperature. For the different H_2 flows, the data show that for both substrate temperatures the H content is lower and the R^* value is higher at a H_2 flow of 0 sccs. Together with the lower refractive index, this implies that the films deposited with 0 sccs H_2 contain a considerable amount of voids. From these observations it is concluded that the films obtained at very low H_2 flows have inferior structural properties compared to those deposited at high H_2 flows. As will be addressed in more detail in Sec. IV A, this behavior can be attributed to the contribution of different plasma species to *a*-Si:H growth. At high H_2 flows, film growth is dominated by SiH_3 radicals which have a relatively low surface reaction probability. At very low H_2 flows on the other hand, there is a large contribution of radicals with surface reaction probabilities close to one. This transition to radicals with a lower surface reactivity when going to higher H_2 flows, is also indicated by the decrease of the surface roughness with increasing H_2 flow as shown in Fig. 6.

Compared to *a*-Si:H deposited by conventional techniques such as rf PECVD, the ETP deposited *a*-Si:H distinguishes itself mainly by the much higher deposition rate. Furthermore, a higher substrate temperature is necessary for the ETP technique to obtain the same refractive index and Si mass density: rf PECVD yields usually dense films at substrate temperatures of 250 °C,[43,46] whereas for the films deposited at high rate by the expanding thermal plasma a substrate temperature over 350 °C is required.[29,31,47] The H content and the microstructure parameter R^* for the ETP films deposited at 250 °C are also higher than for ''optimized'' rf PECVD films which are usually deposited at this substrate temperature. These rf PECVD films contain typically ~10–12 at. % H while the value for $R^* < 0.1$.[43,46]

The H content of the ETP films deposited at 400 °C is lower than for optimized rf PECVD material ($T = \sim 250$ °C) while the R^* value is still higher. Nevertheless, in Sec. III B it will be shown that a substrate temperature of 400 °C yields the optimized film quality for the ETP technique. The difference in substrate temperatures yielding optimum film quality leads however to somewhat different optical and electronic properties between the two optimized materials as will be addressed in Sec. III B.

The last structural property investigated for the very high rate deposited *a*-Si:H is the lattice disorder, which is deduced from the Raman Si–Si TO linewidth. Raman spectra of films deposited with 10 sccs H_2 are given in Fig. 7 for substrate temperatures of 200 and 450 °C. The spectra show only a broad feature at ~475 cm^{-1} indicating that the material is purely amorphous. The half width at half maximum of the Si–Si TO mode is 35 cm^{-1} for the 200 °C sample and 33 cm^{-1} for the 450 °C sample. The corresponding bond-angle distortions[48] are 9° and 8.5°, respectively. These values are also typically found for rf PECVD *a*-Si:H.[49]

B. Optoelectronic film properties

The AM 1.5 photoconductivity σ_{ph} and dark conductivity σ_d of the films are given in Fig. 8. Both σ_{ph} and σ_d are higher for the films deposited at 400 °C, but their ratio σ_{ph}/σ_d (photosensitivity) is lower at this temperature. This lower photosensitivity is mainly due to the higher values of

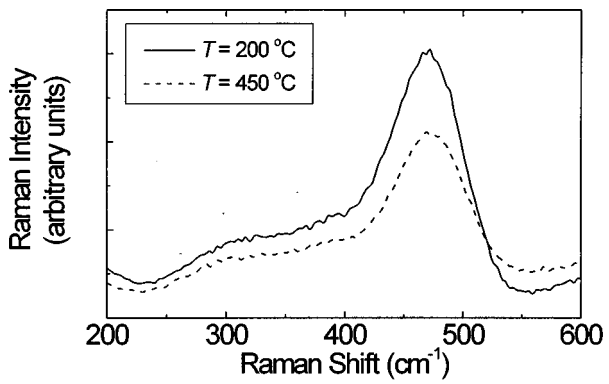

FIG. 7. Raman spectra for films deposited with 10 sccs H_2 at substrate temperatures of 200 and 450 °C.

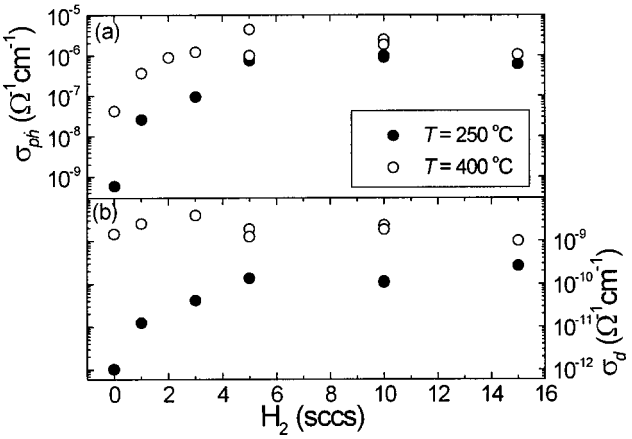

FIG. 8. (a) AM 1.5 photoconductivity $\sigma_{\rm ph}$ (100 mW/cm^2) and (b) dark conductivity σ_d as a function of the H_2 flow in the cascaded arc.

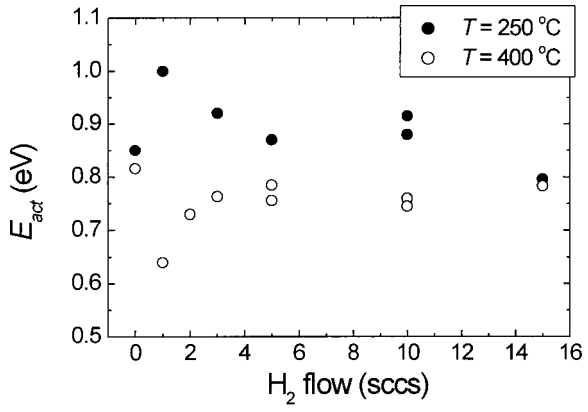

FIG. 9. Activation energy $E_{\rm act}$ of the dark conductivity.

σ_d at 400 °C. Furthermore, it is clear that $\sigma_{\rm ph}$ decreases for decreasing H_2 flow leading to a very small photosensitivity at low H_2 flows. This implies that also the optoelectronic film properties deteriorate for decreasing H_2 flow in the cascaded arc.

In comparison with rf PECVD a-Si:H, the photosensitivity of the ETP films is rather low: $\sim 10^4$ at 250 °C and $\sim 10^3$ at 400 °C. For high quality rf PECVD *a*-Si:H deposited at substrate temperatures around 250 °C, a photosensitivity of $\sim 10^5$ is usually reported, with $\sigma_{\rm ph}$ in the order of $10^{-5}\,\Omega^{-1}\,{\rm cm}^{-1}$ and σ_d preferably $<10^{-10}\,\Omega^{-1}\,{\rm cm}^{-1}$.[43,46] For the ETP films obtained at 250 °C, $\sigma_{\rm ph}$ is about one order of magnitude smaller. This shows that at the substrate temperatures typically used for *a*-Si:H deposition the quality of the very high rate deposited ETP material is indeed inferior. This agrees with the lower Si atomic density obtained at 250 °C. The comparison of the ETP films deposited at 400 °C with rf PECVD films produced at 250 °C is, however, somewhat more complicated. The values of $\sigma_{\rm ph}$ are slightly smaller than for the optimized rf PECVD films, but especially the values of σ_d are higher. The higher values of σ_d can (partially) be attributed to the earlier-mentioned lower H content of the ETP deposited *a*-Si:H. This lower H content leads to a lower optical band gap,[46,50,51] and consequently to a smaller activation energy $E_{\rm act}$ of σ_d and therefore to higher values for σ_d itself. The activation energy of σ_d is given in Fig. 9. The typical value of ~0.75 eV at 400 °C is slightly smaller than the usually reported value of ~0.8 eV for rf PECVD *a*-Si:H. Because σ_d is very sensitive on $E_{\rm act}$ due to the exponential dependence, the smaller value of $E_{\rm act}$ is one reason for the relatively low photosensitivity at 400 °C. For the 250 °C deposited films $E_{\rm act}$ is higher (~0.90 eV) than for rf PECVD films deposited at this temperature, in agreement with their higher H content.

The optical gap has only been determined for the condition with 10 sccs H_2. The Tauc gap $E_{\rm Tauc}$ is 1.67 eV for films deposited at 400 °C, which is indeed lower than the typical values of 1.7–1.8 eV for rf PECVD *a*-Si:H.[43,46] For the ETP films deposited at 250 °C, $E_{\rm Tauc}$ is 1.76 eV. The cubic optical gap $E_{\rm cubic}$ is 1.51 eV for the films deposited at 400 °C, which is about twice the value of $E_{\rm act}(0.75\,{\rm eV})$. This implies that the material does not suffer severely from impurities[43] as also concluded from nuclear analysis of *a*-Si:H films. Furthermore, the lower bandgap leads to a larger absorption coefficient ($\alpha = 3.8\times 10^4\,{\rm cm}^{-1}$ at 2.0 eV), implying that in solar cells with ETP *a*-Si:H thinner intrinsic films can be used.

To obtain more insight into the electronic properties, the electron and hole drift mobility have been investigated by means of TOF measurements for films deposited with 10 sccs H_2. The deposition rate of these films was 10 nm/s.[38] The mobilities for films deposited at 325 and 450 °C are shown in Fig. 10 as a function of the TOF-analysis temperature and for an electric field of $10^4\,{\rm V\,cm}^{-1}$. The hole and electron mobility are very weakly dependent on the electric field.[31,52] For the 325 °C films, the room temperature drift mobilities are 0.70 $\rm cm^2\,V^{-1}\,s^{-1}$ and $3.7\times 10^{-3}\,\rm cm^2\,V^{-1}\,s^{-1}$ for the electrons and holes, respectively, and 0.81 $\rm cm^2\,V^{-1}\,s^{-1}$ and $1.1\times 10^{-2}\,\rm cm^2\,V^{-1}\,s^{-1}$ for the 450 °C films. The increase of both mobilities with increasing substrate temperature clearly shows that the electronic film properties improve with increasing substrate temperature. The activation energies are 0.29 and 0.24 eV for the electrons at 325 and 450 °C, respectively, which is higher than the typical value of 0.15 eV.[53] The activation energy of the hole mobility, which is 0.39 eV for both substrate temperatures, is standard.[53] Very remarkable is that the hole drift mobility of

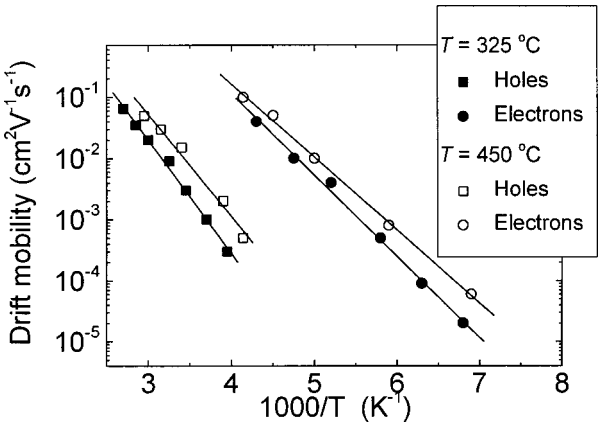

FIG. 10. Electron and hole drift mobility of the *a*-Si:H for an electric field of $10^4\,{\rm V\,cm}^{-1}$. The H_2 flow in the arc was 10 sccs and the substrate temperatures were 325 and 450 °C.

the ETP material at 450 °C is about one order of magnitude larger than for standard *a*-Si:H.[53] The electron drift mobility, however, is about a factor 3–6 smaller. The relatively high hole drift mobility, coupled to the only slightly lower electron drift mobility, results in an increased average carrier mobility and hence a higher recombination rate.[54] This yields a second explanation for the relatively low photosensitivity of the material compared to rf PECVD *a*-Si:H.

Finally, it should be mentioned that also the defect density of the ETP *a*-Si:H deposited at high substrate temperatures is reasonably low. Post-transit photocurrent analysis of the TOF experiments, described in detail in Refs. 31 and 52, yielded a defect density of $\sim 10^{16}\,\mathrm{cm}^{-3}$. In combination with the enhanced hole drift mobility, this suggests that the ETP deposited *a*-Si:H is suitable for the application in solar cells.

C. Solar cells

Attempts on the fabrication of solar cells with an intrinsic *a*-Si:H layer deposited by the expanding thermal plasma have been carried out. The fact that the best film properties are obtained at relatively high substrate temperatures complicates the application of the ETP material in the commonly used *p-i-n* solar cell structure. Deposition of the intrinsic film at substrate temperatures over 300 °C causes severe deterioration of the *p* layer and consequently zero solar cell performance. Therefore, two different, single junction solar cells have been fabricated: a *p-i-n* cell with the *i* layer deposited at 300 °C has been produced in cooperation with the Delft University of Technology, and a *n-i-p* cell with the *i* layer deposited at 400 °C in cooperation with Utrecht University. In the *n-i-p* cell, a thermally stable *n* layer was used as also applied in HWCVD deposited solar cells.[55] For both cells, the doped layers were prepared in rf PECVD chambers, and the vacuum was broken to deposit the intrinsic *a*-Si:H films in the ETP setup. The *i* layers were deposited with a H_2 flow of 10 sccs and at a deposition rate of 7 nm/s. The *p-i-n* cell contained a 10-nm-thick *p* layer deposited on glass with Asahi SnO_2 and a 20-nm-thick *n* layer. For the *n-i-p* cell, a 75 nm thick *n* layer deposited on stainless steel at a substrate temperature of 430 °C has been used. The *p* layer was 30 nm and the cell was finished with a 40-nm-thick indium tin oxide (ITO) top contact. The thickness of the *i* layers was 400 and 500 nm for the *p-i-n* cell and *n-i-p* cell, respectively, while no optimization of these values has taken place.

The performances of the solar cell devices are listed in Table I and the current–voltage curves are given in Fig. 11. The cell deposited at 300 °C had an initial efficiency of 4.1% (under 100 mW/cm^2 AM 1.5 illumination). This *p-i-n* cell suffered already from degradation of the *p* layer as can also be concluded from its relatively low V_{oc}. However, its performance is still better than that of the *n-i-p* cell, which had an efficiency of 3.3%. This is despite the fact that the properties of the individual *i* layer at 400 °C are superior. The lower efficiency can, among other things, be attributed to the fact that for the 400 °C cell the ITO top contact was not optimized for optical transmission. As a reference, the *p-i-n* cells with the *i* layer deposited by rf PECVD and *n-i-p* cells with the *i* layer deposited by HWCVD have record initial efficiencies of 10%[56] and 5.6%,[55] respectively.

TABLE I. Performance of single junction solar cells based on two different cell structures. The intrinsic *a*-Si:H layer has been deposited by the expanding thermal plasma at a rate of 7 nm/s. For the *p-i-n* cell the thickness was 400 nm, for the *n-i-p* cell 500 nm, and the substrate temperatures were 300 and 400 °C, respectively.

	p-i-n cell	*n-i-p* cell
Open circuit voltage V_{oc}	0.61 V	0.72 V
Short circuit current density J_{sc}	14.3 mA/cm^2	11.2 mA/cm^2
Fill-factor FF	0.48	0.42
Efficiency η	4.1%	3.3%

Considering the fact that no optimization of the solar cells in their entirety has been carried out, such as tuning of the properties of the doped layers and a refinement of the thickness of the intrinsic *a*-Si:H layer, these preliminary results on solar cells deposited at a rate of 7 nm/s are promising. Furthermore, we note that transport through air was inevitable (total air exposure time >12 h) and that no light trapping and no special back reflection enhancement techniques were applied.

IV. DISCUSSION

A. Relation between the film properties and the growth precursors

In the previous sections, it has been shown that the film properties obtained at no or very low H_2 flows are inferior to those obtained at H_2 flows within the range of 5–15 sccs. This behavior can be related to a change in the plasma processes and film growth precursors when the H_2 flow is varied. By detailed investigations using several plasma diagnostics[32,34,35,37] it is found that for the different H_2 flows two different regions can be distinguished with respect to the SiH_4 dissociation process. At low H_2 flows, SiH_4 is mainly dissociated by reactions induced by ions emanating from the plasma source. By means of dissociative charge transfer reactions with ions and dissociative recombination reactions with electrons this leads to a considerable production of SiH_x radicals ($x \leqslant 2$).[34,35,37] These radicals have a high (surface)

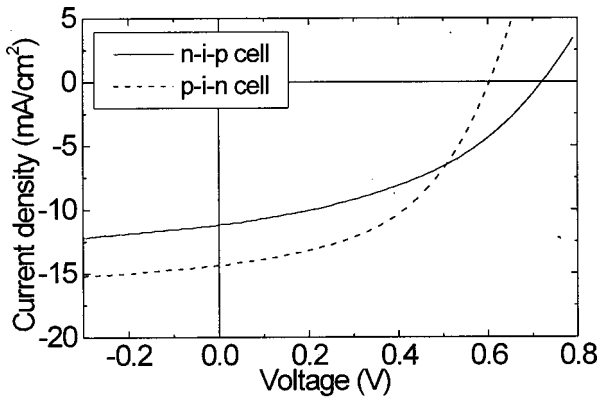

FIG. 11. *I–V* curves for solar cells with an intrinsic *a*-Si:H layer deposited by the expanding thermal plasma at a rate of 7 nm/s. During the deposition of the intrinsic layer the H_2 flow in the arc was 10 sccs and the substrate temperature was 300 and 400 °C for the *p-i-n* and *n-i-p* cell, respectively.

reactivity, and they contribute either directly to film growth or react first with SiH_4 to create reactive polysilane radicals [such as $Si_2H_x(x \leqslant 4)$, etc.][57] before contributing to growth. When the H_2 admixture is increased, the flow of ions from the plasma source reduces drastically, whereas the flow of atomic H from the source increases. This leads to more hydrogen abstraction reactions between SiH_4 and H and consequently to an increasing contribution of SiH_3 to film growth. For H_2 flows $\gtrsim$7.5 sccs, film growth is by far dominated by SiH_3 (contribution is estimated at $\sim$90%).[37] Under these conditions the amount of H emanating from the source is almost fully consumed[37] and the flux of SiH_3 towards the *a*-Si:H surface is much larger than the flux of H.[58] The contribution of Si containing positive ions to film growth is less than 10%[35,37] and rather independent of the H_2 flow.[35] Despite the fact that at low H_2 flows SiH_4 dissociation is governed by ions, fast dissociative recombination reactions of the ions with electrons under these conditions lead to a strong reduction of the contribution of the ions at low H_2 flows.[37]

The transition to dominantly SiH_3 when increasing the H_2 flow is corroborated by the dependence of the overall surface reaction probability on the H_2 flow. This overall surface reaction probability depends on the fluxes of different reactive species to the film and on each of their particular surface reaction probabilities. The overall surface reaction probability decreases from $\sim$0.5 to $\sim$0.3 when increasing the H_2 flow from 0 to 15 sccs.[36,37] At the high H_2 flows, the overall surface reaction probability of $\sim$0.3 approaches the values of the surface reaction probability proposed for SiH_3(0.2–0.3).[36] At low H_2 flows, there is apparently a significant contribution of reactive $SiH_x(x \leqslant 2)$ and polysilane radicals. For these radicals, values of the surface reaction probability within the range of 0.6–1 have been proposed.[36]

From these results, the poorer *a*-Si:H film quality obtained at low H_2 flows can be understood. Radicals with a high surface reaction probability lead easily to a high surface roughness and columnar film growth because they stick (almost) immediately at their position of impact on the surface (the ''microscopic-shadowing'' effect).[59] Radicals with a lower surface reaction probability on the other hand, can have multiple reflections on the surface before they actually stick. Radicals such as SiH_3 are therefore capable of filling up so-called ''valleys'' at the surface[59] causing smoother film growth. (On this point we disagree with Doughty *et al.*[60] Without underrating the importance of surface diffusion, a radical that can undergo several reflections has certainly a larger probability of ending up at the ''bottom of a valley.'') The decreasing surface roughness for increasing H_2 flow is thus in perfect agreement with the increasing contribution of SiH_3. Since voids are more easily incorporated when the surface is rough, a higher contribution of very reactive radicals explains the lower Si atomic density and higher void fraction at very low H_2 flows.

The improvement of the optoelectronic properties with increasing H_2 flow can be understood from the improvement of the electronic transport properties with increasing film density. Porous films are obviously also more susceptible to oxidation when exposed to air. It is also expected that the defect density of the films depends on the species contributing to growth. Furthermore, σ_{ph} and σ_d show somewhat more dependence on the H_2 flow than the structural film properties, especially at a substrate temperature of 400 °C. This suggests that it is easier to compensate for poor structural properties (as caused by the growth precursors) by using high substrate temperatures than for poor electronic performance.

Because the film properties do not show a correlation with the contribution of the cationic Si clusters, no relation between their contribution and the film properties can be extracted from the data. However, it is not excluded that these ions have important implications for the film quality, as has also been discussed in Refs. 33 and 35. Despite the fact that the contribution of the ions is within the range of 5%–9%, these H poor and compact clusters can easily affect the defect density: their contribution is much larger than the defect density in high quality *a*-Si:H that is in the order of 10^{-6}–10^{-7} of the Si atomic density.[43,46]

It can be concluded that the type of species contributing to *a*-Si:H growth has important implications for the film properties finally obtained. It has been shown that the quality of the *a*-Si:H with respect to solar cell applications improves with an increasing contribution of SiH_3. Such a relation is already generally accepted for *a*-Si:H produced at the commonly used deposition rates, but here this relation is also found for very high rate deposited *a*-Si:H. It is important to realize that the film quality, in terms of electronic properties, is not necessarily directly related to the contribution of SiH_3. Film properties such as the defect density can also completely be determined by a (small) contribution of other species than SiH_3. Furthermore, the results obtained with the ETP technique imply that a dominant contribution of SiH_3 only is not sufficient to obtain high quality *a*-Si:H at high deposition rates. Under these conditions, also higher substrate temperatures are required to obtain films with a sufficiently high mass density. This might be related to the high deposition rate itself and/or the absence of a (sufficient) ion bombardment of the film during deposition as will be discussed in the following section.

B. Comparison with *a*-Si:H deposited by other techniques

In Sec. III, the ETP deposited *a*-Si:H has been compared to rf PECVD *a*-Si:H, typically deposited at substrate temperatures between 200 and 300 °C. In this section, we will also compare the material with *a*-Si:H deposited by other techniques, where in some cases either the material properties or the process conditions show striking similarities. Although such a comparison is afflicted with differences in analyzed film parameters, method of analysis, etc., it is still worth trying to come to some general insights regarding the growth and properties of *a*-Si:H.

First of all, the relation between the deposition rate and substrate temperature is considered. In the present study, it has been shown that relatively high substrate temperatures are necessary to obtain dense films with a sufficiently low R^*. This requirement can be caused by the high deposition

rate itself[47] but it might also be related to the absence of energetic ion bombardment during deposition (sheath potential <2 eV).[33,34] That it is possible to deposit high quality *a*-Si:H at lower substrate temperatures when sufficient ion bombardment takes place is also suggested by Abelson.[61] Moreover, a relation between the ion energy and both the film density and R^* is indicated by the data of Hamers *et al.*[62] Using rf and VHF PECVD, it was shown that dense films with $R^*<0.1$ were obtained when 5 eV ion energy was available per Si atom deposited. This observation is consistent with the fact that films with reasonable properties can be obtained at 3 nm/s by rf PECVD when depositing at the cathode and using somewhat higher substrate temperatures (350 °C) than usually.[3] The HWCVD technique on the other hand, is capable of producing very dense films with $R^*=0$ at deposition rates up to 2 nm/s and at relatively low substrate temperatures while ion bombardment is absent.[20,23,24,26] This absence of energetic ion bombardment can possibly be compensated by a large flux of ''energetic'' H that is thermalized at the filament.[20] Furthermore, it should be noted that the substrate temperatures reported for HWCVD are not always reliable because accurate temperature control is difficult due to the presence of a hot filament.[63,64] In some cases, only the substrate temperature prior to deposition is reported.[65]

Another important effect associated with ion bombardment is the enhancement of the electron and hole drift mobility as reported for rf PECVD *a*-Si:H for ion energies within an extremely narrow window around 20 eV($T=250$ °C).[66,67] The exact values of the mobilities have been under discussion in Refs. 53 and 68. The enhancement of the mobilities can possibly be associated with the ion-energy effects observed in Si^+ beam epitaxy by Rabalais *et al.*[69] Low defect density crystalline silicon was obtained for ion energies within a very narrow window ($\sim 20\pm 10$ eV) at low substrate temperatures (160 °C). For higher temperatures this window broadened out, particularly at the low-energy side. These observations also suggest that ion bombardment can be interchanged with substrate temperature, at least as long as the typical ion energy is not much larger than the displacement threshold energy causing deleterious effects.

Going back to HWCVD, for the *a*-Si:H produced by this technique some very interesting properties have been observed. Mahan *et al.*[20] have shown that no severe deterioration of the film properties takes place when going to high substrate temperatures and to low H concentrations in the films (down to $<1\%$ for $T>400$ °C). For increasing substrate temperature, both σ_{ph} and the electron drift mobility[70] showed only a slight decrease, while an improved stability against light-induced degradation was obtained for films with a H content of 2–3 at. % ($T=400$ °C prior to deposition).[65] Furthermore, E_{Tauc} and σ_d of the material remained, respectively, high and low when going to low H concentrations.

In comparison with the ETP *a*-Si:H films deposited at 400 °C, the lower H content and the value of $R^*=0$ for the HWCVD films are remarkable. Because the substrate temperature was 400 °C prior to deposition, this difference suggests that the substrate temperature during the deposition of the HWCVD films was considerably higher than 400 °C. Furthermore, some significant differences have been reported for films deposited by different HWCVD reactors under similar circumstances. The drastic decrease in H content with increasing substrate temperature has been reproduced in several other studies,[64,71] but Feenstra *et al.* found film properties improving with increasing substrate temperature while the H content remained high (9.5 at. %) up to 430 °C.[21] This material showed also no improved stability compared to rf PECVD *a*-Si:H and values of $R^*\geqslant 0.1$ were reported.[72] Heintze *et al.* reported similar R^* values for films containing 4 at. % H which were obtained at a substrate temperature of 400 °C. These films showed only a slightly improved stability.[71]

Also the observation by Mahan *et al.*[20] that both E_{Tauc} and σ_d remained constant when going to films with a low H concentration is remarkable. This behavior is in contrast with the observations for ETP deposited *a*-Si:H, but also with the observations for HWCVD *a*-Si:H films reported by Nelson *et al.*[64] and Heintze *et al.*[71] Mahan *et al.* has attributed the fact that E_{Tauc} remained constant at a relatively high value when going to low H concentrations to improved structural ordering in the HWCVD films.[20,27]

Regarding the improved structural ordering in low H content HWCVD *a*-Si:H,[20,27] there might be some similarities with the ETP deposited *a*-Si:H. Although speculative, the higher hole drift mobility in the ETP material as well as the appearance of a steep edge in the band tail states[31] might suggest also a different network bonding, while the enhanced hole drift mobility might be related with the relatively large ambipolar diffusion length in the low H content HWCVD *a*-Si:H films.[20] For the moment, it can only be mentioned that both techniques yield *a*-Si:H with similar values for the half width at half maximum of the Raman Si–Si TO mode,[27] values which are also typically found for rf PECVD *a*-Si:H.

Another aspect related to R^*, is the fact that H bonded as SiH_2 in the film has been linked with the contribution of higher silane related chemical species and subsequently with light-induced degradation of *a*-Si:H.[73] The fact that R^* increases with increasing deposition rate,[51,74,75] has been attributed to the higher contribution of these species to film growth, because these kind of species are more created at higher plasma power and/or pressure in rf PECVD (the method usually applied to increase the deposition rate).[73] For the optimized plasma conditions in the expanding thermal plasma (i.e., high H_2 flow), film growth is dominated by SiH_3 and only a very small fraction of higher silanes has been observed.[32,35] The R^* value is nevertheless relatively high, especially at 250 °C. Furthermore, no strong dependence of R^* on the H_2 flow has been observed (see Fig. 5), while the contribution of polysilane radicals presumably increases significantly when going to low H_2 flows.

The ETP technique has some similarities with other remote plasmas, such as the microwave operated ''remote hydrogen plasma'' (RHP)[12] and the H_2 operated electron cyclotron resonance plasma (H–ECR).[19] These plasmas use also H generated in a H_2 operated source to dissociate SiH_4, and therefore film growth is presumably also dominated by SiH_3 in these techniques. Furthermore, in these plasma also less ion bombardment takes place (this is to a smaller extent valid

for H–ECR)[76] and high substrate temperatures ($T=\sim 400\,^{\circ}\mathrm{C}$) are typically used as well. The RHP technique yields however a relatively high H content at this temperature (10 at. %)[12] while $R^*=\sim 0$.[77] For H–ECR the relatively high E_{Tauc} of 1.74 eV at 450 °C[76] suggests also a relatively high H content. Furthermore, it is suggested that for both techniques there is a relatively high H flux during deposition. It is therefore intriguing that, under similar circumstances as for HWCVD, also an improved stability for the material has been reported.[12,19] The HWCVD material, however, has a H content of 2–3 at. %. with $R^*=\sim 0$,[20] while the SiH_4 dissociation process and dominant growth precursors are also very different. The SiH_4 is decomposed at a filament yielding mainly Si and H atoms.[63] These radicals can subsequently react with SiH_4 before reaching the substrate. The probability for these reactions, however, is limited due to the relatively low SiH_4 pressure and small distance between filament and substrate (typically $\leqslant$5 cm). It is expected that a considerable fraction of the (hot) Si atoms can react with SiH_4 (to mainly H_2SiSiH_2),[63,78] but this is less evident for H. It is rather improbable that H reacts to SiH_3 in the gas phase and the proposed scheme that SiH_3 is created at the *a*-Si:H surface by H (i.e., H creates a surface dangling bond by H abstraction and this surface dangling bond abstracts subsequently a H atom from SiH_4)[78] is also unlikely because of the very low reactivity of SiH_4 with pristine crystalline Si surfaces.[79,80] It can therefore be excluded that in HWCVD SiH_3 contributes dominantly to film growth. This shows that a dominant contribution of SiH_3 is not a necessary condition for high quality *a*-Si:H growth.

V. CONCLUSION

The film properties of *a*-Si:H deposited using the expanding thermal plasma have been investigated for different operating conditions of the plasma source and for two different substrate temperatures. It has been shown that this technique is capable of depositing low-defect density *a*-Si:H at deposition rates up to 10 nm/s for a substrate temperature of 400 °C and a relatively high H_2 flow in the cascaded arc plasma source. The *a*-Si:H obtained for these conditions is suitable for application in solar cells but it has somewhat different properties than rf PECVD *a*-Si:H. The substrate temperature of 400 °C, necessary to obtain dense films at high deposition rates, leads to a relatively low H content of 6–7 at. % and a relatively high microstructure parameter R^* of 0.2. The films have a small Tauc band gap ($\sim$1.67 eV) and a relatively small activation energy of the dark conductivity ($\sim$0.75 eV). This is related with the low H content of the films and it explains, at least partially, the relatively high dark conductivity ($\sim 2\times 10^{-9}\,\Omega^{-1}\,\mathrm{cm}^{-1}$) of the films. The photoconductivity of the material ($\sim 4\times 10^{-6}\,\Omega^{-1}\,\mathrm{cm}^{-1}$) is slightly lower than for optimized rf PECVD *a*-Si:H. This can most probably be attributed to the enhanced hole drift mobility of the material which is about a factor of 10 higher than for optimized rf PECVD *a*-Si:H. The enhanced hole drift mobility without the equivalent reduction of the electron drift mobility leads to enhanced recombination.

The preliminary results on the solar cells with the *i* layer deposited at 7 nm/s by the expanding thermal plasma show also the potential of very high rate deposited *a*-Si:H. A simple *p-i-n* cell with the *i* layer deposited at 300 °C yielded an efficiency of 4.1%, despite thermal degradation of the *p* layer and a not fully optimized intrinsic *a*-Si:H layer. Moreover, the cell thickness was not optimized and air exposure was inevitable. The *n-i-p* cell, with a thermally stable *n* layer and with higher quality intrinsic *a*-Si:H deposited at 400 °C, yielded an efficiency of 3.3%, despite a nonoptimized ITO top contact. These results are encouraging for further solar cell optimization, which will be done in a recently developed solar cell deposition system consisting of a rf PECVD reactor, an expanding thermal plasma reactor, and a sample transfer chamber.

The film properties obtained for the different operating conditions of the plasma source have also been related to the SiH_4 dissociation reactions and species contributing to film growth. The improvement of the properties with increasing H_2 flow added to the Ar in the cascaded arc plasma source can be attributed to an increasing contribution of SiH_3 to film growth. The optimum film quality is obtained for conditions in which SiH_3 is by far dominant (contribution SiH_3 is estimated at $\sim$90%), while conditions with a high contribution of very reactive (poly)silane radicals lead to inferior properties. The high surface reaction probability of these radicals leads to a high surface roughness and a low film density.

ACKNOWLEDGMENTS

The authors greatly acknowledge H.-Z. Song from the University of Leuven for performing the TOF measurements, R. E. I. Schropp and C. H. M. van de Werf from Utrecht University, and E. J. Geluk, B. S. Girwar, and R. A. C. M. M. van Swaaij of the Delft University of Technology for the production and testing of the solar cells. M. J. F. van de Sande, A. B. M. Hüsken, and H. M. M. de Jong are thanked for their skilful technical assistance. This work was supported by the Netherlands Organization for Scientific Research (NWO), The Netherlands Foundation for Fundamental Research on Matter (FOM), and The Netherlands Agency for Energy and the Environment (NOVEM).

[1] J. Perrin, P. Roca i Cabarrocas, B. Allain, and J.-M. Friedt, Jpn. J. Appl. Phys., Part 1 **27**, 2041 (1988).
[2] P. Roca i Cabarrocas, J. Non-Cryst. Solids **164–166**, 37 (1993).
[3] S. Will, H. Mell, M. Poschenrieder, and W. Fuhs, J. Non-Cryst. Solids **227–230**, 29 (1998).
[4] J. C. Knights, R. A. Lujian, M. P. Rosenblum, R. A. Street, D. K. Biegelsen, and J. A. Reimer, Appl. Phys. Lett. **38**, 331 (1981).
[5] H. Meiling, J. Bezemer, R. E. I. Schropp, and W. F. van der Weg, Mater. Res. Soc. Symp. Proc. **467**, 459 (1997).
[6] W. Futako, T. Takagi, T. Nishimoto, M. Kondo, I. Shimizu, and A. Matsuda, Jpn. J. Appl. Phys., Part 1 **38**, 4534 (1999).
[7] M. Heintze and R. Zedlitz, J. Non-Cryst. Solids **164–166**, 55 (1993).
[8] W. G. J. H. M. van Sark, J. Bezemer, E. M. B. Heller, M. Kars, and W. F. van der Weg, Mater. Res. Soc. Symp. Proc. **377**, 3 (1995).
[9] U. Kroll, J. Meier, P. Torres, J. Pohl, and A. Shah, J. Non-Cryst. Solids **227–230**, 68 (1998).
[10] W. G. J. H. M. van Sark, J. Bezemer, R. van der Heijden, and W. F. van der Weg, Mater. Res. Soc. Symp. Proc. **420**, 21 (1996).
[11] S. J. Jones, X. Deng, T. Liu, and M. Izu, Mater. Res. Soc. Symp. Proc. **507**, 113 (1998).
[12] N. M. Johnson, C. E. Nebel, P. V. Santos, W. B. Jackson, R. A. Street, K.

S. Stevens, and J. Walker, Appl. Phys. Lett. **59**, 1443 (1991).
[13] J. M. Jasinski, J. Vac. Sci. Technol. A **13**, 1935 (1995).
[14] M. Goto, H. Toyoda, M. Kitagawa, T. Hirao, and H. Sugai, Jpn. J. Appl. Phys., Part 1 **36**, 3714 (1997).
[15] J. A. Theil and G. Powell, J. Appl. Phys. **75**, 2652 (1994).
[16] K. Yokota, M. Takada, Y. Ohno, and S. Katayama, J. Appl. Phys. **72**, 1188 (1992).
[17] M. Kitagawa, K. Setsune, Y. Manabe, and T. Hirao, Jpn. J. Appl. Phys., Part 1 **27**, 2026 (1988).
[18] M. Zhang, Y. Nakayama, S. Nonoyama, and S. Wakita, J. Non-Cryst. Solids **164–166**, 63 (1993).
[19] V. L. Dalal, T. Maxson, R. Girvan, and S. Haroon, Mater. Res. Soc. Symp. Proc. **467**, 813 (1997).
[20] A. H. Mahan, J. Carapella, B. P. Nelson, R. S. Crandall, and I. Balberg, J. Appl. Phys. **69**, 6728 (1991).
[21] K. F. Feenstra, C. H. M. van der Werf, E. C. Molenbroek, and R. E. I. Schropp, Mater. Res. Soc. Symp. Proc. **467**, 645 (1997).
[22] A. H. Mahan *et al.*, Mater. Res. Soc. Symp. Proc. **507**, 119 (1998).
[23] P. Alpuim, V. Chu, and J. P. Conde, J. Appl. Phys. **86**, 3812 (1999).
[24] M. Vanecek, Z. Remes, J. Fric, R. S. Crandall, and A. H. Mahan, *Proceedings of the 12th European Photovoltaic Solar Energy Conference*, Amsterdam, The Netherlands, 1994, p. 354.
[25] D. Kwon, J. D. Cohen, B. P. Nelson, and E. Iwaniczko, Mater. Res. Soc. Symp. Proc. **377**, 301 (1995).
[26] Y. Wu, J. T. Stephen, D. X. Han, J. M. Rutland, R. S. Crandall, and A. H. Mahan, Phys. Rev. Lett. **77**, 2049 (1996).
[27] A. H. Mahan, D. L. Williamson, and T. E. Furtak, Mater. Res. Soc. Symp. Proc. **467**, 657 (1997).
[28] R. S. Crandall, X. Liu, and E. Iwaniczko, J. Non-Cryst. Solids **227–230**, 23 (1998).
[29] R. J. Severens, M. C. M. van de Sanden, H. J. M. Verhoeven, J. Bastiaanssen, and D. C. Schram, Mater. Res. Soc. Symp. Proc. **420**, 341 (1996).
[30] W. M. M. Kessels, A. H. M. Smets, B. A. Korevaar, G. J. Adriaenssens, M. C. M. van de Sanden, and D. C. Schram, Mater. Res. Soc. Symp. Proc. **557**, 25 (1999).
[31] B. A. Korevaar, G. J. Adriaenssens, A. H. M. Smets, W. M. M. Kessels, H.-Z. Song, M. C. M. van de Sanden, and D. C. Schram, J. Non-Cryst. Solids **266–269**, 380 (2000).
[32] M. C. M. van de Sanden, R. J. Severens, W. M. M. Kessels, R. F. G. Meulenbroeks, and D. C. Schram, J. Appl. Phys. **84**, 2426 (1998); **85**, 1243 (1999).
[33] W. M. M. Kessels, C. M. Leewis, A. Leroux, M. C. M. van de Sanden, and D. C. Schram, J. Vac. Sci. Technol. A **17**, 1531 (1999).
[34] M. C. M. van de Sanden, W. M. M. Kessels, R. J. Severens, and D. C. Schram, Plasma Phys. Controlled Fusion **41**, A365 (1999).
[35] W. M. M. Kessels, C. M. Leewis, M. C. M. van de Sanden, and D. C. Schram, J. Appl. Phys. **86**, 4029 (1999).
[36] W. M. M. Kessels, M. C. M. van de Sanden, R. J. Severens, and D. C. Schram, J. Appl. Phys. **87**, 3313 (2000).
[37] W. M. M. Kessels, M. C. M. van de Sanden, and D. C. Schram, J. Vac. Sci. Technol. **18**, 2153 (2000).
[38] With a H_2 flow of 10 sccs typically a deposition rate of 7–8 nm/s is obtained. However, due to a drift in the SiH_4 mass flow controller, some measurements, such as the presented TOF analysis, have been performed on films deposited at somewhat higher rates (~10 nm/s). As shown in a separate study this has no significant influence on the film properties nor on the plasma composition (Ref. 37).
[39] J. W. A. M. Gielen, W. M. M. Kessels, M. C. M. van de Sanden, and D. C. Schram, J. Appl. Phys. **82**, 2643 (1996).
[40] A. H. M. Smets, M. C. M. van de Sanden, and D. C. Schram, Thin Solid Films **343–344**, 281 (1999).
[41] A. H. M. Smets, M. C. M. van de Sanden, and D. C. Schram, J. Appl. Phys. **88**, 6388 (2000).
[42] W. M. M. Kessels, M. C. M. van de Sanden, R. J. Severens, L. J. Van IJzendoorn, and D. C. Schram, Mater. Res. Soc. Symp. Proc. **507**, 529 (1998).
[43] R. E. I. Schropp and M. Zeman, *Amorphous and Microcrystalline Silicon Solar Cells: Modeling, Materials and Device Technology* (Kluwer Academic, Boston, 1998).
[44] T. Tiedje, J. M. Cebulka, D. L. Morel, and B. Abeles, Phys. Rev. Lett. **46**, 1425 (1981).
[45] R. J. Severens, G. J. H. Brussaard, M. C. M. van de Sanden, and D. C. Schram, Appl. Phys. Lett. **67**, 491 (1995).
[46] W. Luft and Y. S. Tsuo, *Hydrogenated Amorphous Silicon Alloy Deposition Processes* (Marcel Dekker, New York, 1993).
[47] W. M. M. Kessels, R. J. Severens, M. C. M. van de Sanden, and D. C. Schram, J. Non-Cryst. Solids **227–230**, 133 (1998).
[48] D. Beeman, R. Tsu, and M. F. Thorpe, Phys. Rev. B **32**, 874 (1985).
[49] A. H. Mahan, in *Properties of Amorphous Silicon and Its Alloys*, edited by Tim Searle (Inspec, London, 1998), p. 39.
[50] N. Maley and J. S. Lannin, Phys. Rev. B **36**, 1146 (1987).
[51] C. Manfredotti, F. Fizzotti, M. Boero, P. Pastorino, P. Polesello, and E. Vittone, Phys. Rev. B **50**, 18046 (1994).
[52] G. J. Adriaenssens, H.-Z. Song, V. I. Arkhipov, E. V. Emelianova, W. M. M. Kessels, A. H. M. Smets, B. A. Korevaar, and M. C. M. van de Sanden, J. Optoelectronics and Advanced Materials **2**, 31 (2000).
[53] G. J. Adriaenssens, in *Properties of Amorphous Silicon and Its Alloys*, edited by Tim Searle (Inspec, London, 1998), p. 199.
[54] H. Dersch, L. Schweitzer, and J. Stuke, Phys. Rev. B **28**, 4678 (1983).
[55] K. F. Feenstra, J. K. Rath, C. H. M. van der Werf, Z. Hartman, and R. E. I. Schropp, *Proceedings of the 2nd World Conference on Photovoltaic Energy Conversion*, Vienna, Austria, 1998, p. 956.
[56] M. Zeman, R. A. C. M. M. van Swaaij, E. Schroten, L. L. A. Vosteen, and J. W. Metselaar, Mater. Res. Soc. Symp. Proc. **507**, 409 (1998).
[57] J. Perrin, O. Leroy, and M. C. Bordage, Contrib. Plasma Phys. **36**, 1 (1996).
[58] W. M. M. Kessels, A. Leroux, M. G. H. Boogaarts, J. P. M. Hoefnagels, M. C. M. van de Sanden, and D. C. Schram, J. Vac. Sci. Technol. A (March/April 2001).
[59] A. Gallagher, Mater. Res. Soc. Symp. Proc. **70**, 3 (1986); A. Gallagher, Int. J. Solar Energy **5**, 311 (1988).
[60] D. A. Doughty, J. R. Doyle, G. H. Lin, and A. C. Gallagher, J. Appl. Phys. **67**, 6220 (1990).
[61] J. R. Abelson, Appl. Phys. A: Solids Surf. **56**, 493 (1993).
[62] E. A. G. Hamers, W. G. J. H. M. van Sark, J. Bezemer, H. Meiling, and W. F. van der Weg, J. Non-Cryst. Solids **226**, 205 (1998).
[63] J. Doyle, R. Robertson, G. H. Lin, M. Z. He, and A. Gallagher, J. Appl. Phys. **64**, 3215 (1988).
[64] B. P. Nelson, Q. Wang, E. Iwaniczko, A. H. Mahan, and R. S. Crandall, Mater. Res. Soc. Symp. Proc. **507**, 927 (1998).
[65] A. H. Mahan (private communication).
[66] G. Ganguly and A. Matsuda, Mater. Res. Soc. Symp. Proc. **336**, 7 (1994).
[67] K. Kato, S. Iizuka, G. Ganguly, T. Ikeda, A. Matsuda, and N. Sato, Jpn. J. Appl. Phys., Part 1 **36**, 4547 (1997).
[68] J. Kocka, H. Stuchlikova, A. Fejfar, G. Ganguly, I. Sakata, A. Matsuda, and G. Juska, J. Non-Cryst. Solids **227–230**, 229 (1998).
[69] J. W. Rabalais, A. H. Al-Bayati, K. J. Boyd, D. Marton, J. Kulik, Z. Zhang, and W. K. Chu, Phys. Rev. B **53**, 10781 (1996).
[70] S. Dong, Y. Tang, R. Braunstein, R. S. Crandall, B. P. Nelson, and A. H. Mahan, J. Appl. Phys. **82**, 702 (1997); see also comments on electron drift mobility in Ref. 52.
[71] M. Heintze, R. Zedlitz, H. N. Wanka, and M. B. Schubert, J. Appl. Phys. **79**, 2699 (1996).
[72] K. F. Feenstra, Ph.D. thesis, Utrecht University, The Netherlands, 1998.
[73] T. Takagi, R. Hayashi, A. Payne, W. Futako, T. Nishimoto, M. Takai, M. Kondo, and A. Matsuda, Mater. Res. Soc. Symp. Proc. **557**, 105 (1999).
[74] T. Takagi, K. Takechi, Y. Nakagawa, Y. Watabe, and S. Nishida, Vacuum **51**, 751 (1998).
[75] K. Maeda, I. Umezu, and H. Ishizuka, Phys. Rev. B **55**, 4323 (1997).
[76] R. D. Knox, V. Dalal, B. Moradi, and G. Chumanov, J. Vac. Sci. Technol. A **11**, 1896 (1993).
[77] S. E. Ready, J. B. Boyce, N. M. Johnson, J. Walker, and K. S. Stevens, Mater. Res. Soc. Symp. Proc. **192**, 127 (1990).
[78] E. C. Molenbroek, A. H. Mahan, E. J. Johnson, and A. C. Gallagher, J. Appl. Phys. **79**, 7278 (1996).
[79] S. M. Gates, B. A. Scott, D. B. Beach, R. Imbihl, and J. E. Demuth, J. Vac. Sci. Technol. A **5**, 628 (1987).
[80] L.-Q. Xia, M. E. Jones, N. Maity, and J. R. Engstrom, J. Vac. Sci. Technol. A **13**, 2651 (1995).